Characterization of complex polyether polyols using comprehensive two-dimensional liquid chromatography hyphenated to high-resolution mass spectrometry

Groeneveld, G.; Dunkle, M.N.; Rinken, M.; Gargano, A.F.G.; de Niet, A.; Pursch, M.; Mes, E.P.C.; Schoenmakers, P.J.

DOI
10.1016/j.chroma.2018.07.054

Publication date
2018

Document Version
Final published version

Published in
Journal of Chromatography A

Journal of Chromatography A, 1569 (2018) 128–138

Contents lists available at ScienceDirect

Journal of Chromatography A

journal homepage: www.elsevier.com/locate/chroma

Characterization of complex polyether polyols using comprehensive two-dimensional liquid chromatography hyphenated to high-resolution mass spectrometry

Gino Groeneveld[a,*], Melissa N. Dunkle[b], Marian Rinken[c], Andrea F.G. Gargano[a,d], Ayako de Niet[a], Matthias Pursch[c], Edwin P.C. Mes[b], Peter J. Schoenmakers[a]

[a] University of Amsterdam, Van't Hoff Institute for Molecular Sciences, Science Park 904, 1098 XH Amsterdam, The Netherlands
[b] Dow Benelux B.V., Analytical Science, P.O. Box 48, 4530 AA Terneuzen, The Netherlands
[c] Dow Deutschland Anlagengesellschaft mbH, Analytical Sciences, P.O. Box 1120, 21677 Stade, Germany
[d] Vrije Universiteit Amsterdam, Amsterdam Institute for Molecules, Medicines and Systems, de Boelelaan 1083, 1081HV Amsterdam, The Netherlands

ARTICLE INFO

Article history:
Received 25 April 2018
Received in revised form 22 June 2018
Accepted 17 July 2018
Available online 18 July 2018

Keywords:
Comprehensive two-dimensional liquid chromatography
LC × LC-HRMS
Castor oil ethoxylates
Biobased polyols
EO/PO random copolymers
Blended formulations

ABSTRACT

Polyether polyols are often used in formulated systems, but their complete characterization is challenging, because of simultaneous heterogeneities in chemical composition, molecular weight and functionality. One-dimensional liquid chromatography–mass spectrometry is commonly used to characterize polyether polyols. However, the separation power of this technique is not sufficient to resolve the complexity of such samples entirely.

In this study, comprehensive two-dimensional liquid chromatography hyphenated with high-resolution mass spectrometry (LC × LC-HRMS) was used for the characterization of (*i*) castor oil ethoxylates (COEs) reacted with different mole equivalents of ethylene oxide and (*ii*) a blended formulation consisting of glycerol ethoxylate, glycerol propoxylate and glycerol ethoxylate-*random*-propoxylate copolymers. Retention in the first (hydrophilic-interaction-chromatography) dimension was mainly governed by degree of ethoxylation, while the second reversed-phase dimension resolved the samples based on degree of propoxylation (blended formulation) or alkyl chain length (COEs). For different COE samples, we observed the separation of isomer distributions of various di-, tri- and tetra-esters, and such positional isomers were studied by tandem mass spectrometry (LC–MS/MS). This revealed characteristic fragmentation patterns, which allowed discrimination of the isomers based on terminal or internal positioning of the fatty-acid moieties and provided insight in the LC × LC retention behavior of such species.

1. Introduction

Polyether polyols are key components in the production of polyurethane products. Other application fields include coatings, adhesives, sealants, synthetic lubricants and functional fluids [1]. They are produced by reacting compounds containing one or more active hydrogens (*e.g.* water, glycerol, alkyl alcohols, fatty acids, *etc.*) with organic oxides, such as ethylene oxide (EO) or propylene oxide (PO), in the presence of a base catalyst [2]. The resulting polyether polyols can have a high degree of complexity due to distributions with regard to functionality type (FTD), molecular weight (MWD), chemical composition (CCD), monomer sequence (MSD) and other factors, such as homopolymer/copolymer content. Furthermore, those polyether polyols are often used in formulated systems, increasing the complexity of such samples. Complex formulations may include mixtures of different homopolymers, copolymers (random and/or block-copolymers), or both homo- and copolymers. In addition, a complex formulation can be formed by using a starter feed containing multiple initiators varying in functionality. A unique feedstock for biobased polyols is castor oil (derived from the castor plant), since it contains a high amount of ricinoleic acid (12-hydroxyoleic acid), which contains an additional hydroxyl group in comparison with other fatty acids [1,2]. Through hydrolysis, various free fatty acids, water and glycerol are obtained from the raw material. This ultimately results in a very complex sample when reacted with EO.

Because of the heterogeneity of the sample, data from multiple analytical techniques are often combined and used to characterize polyether polyol formulations. Nuclear-magnetic-resonance (NMR) spectroscopy [3] and matrix-assisted laser desorption/ionization mass spectrometry (MALDI-MS) [4] have been shown to provide details on the initiators used and/or the

* Corresponding author.
E-mail address: G.Groeneveld@uva.nl (G. Groeneveld).

https://doi.org/10.1016/j.chroma.2018.07.054

chemical composition. However, liquid chromatography (LC) and LC hyphenated with mass spectrometry (LC—MS) [5] are the most frequently used techniques to acquire the necessary compositional information, due to the high sensitivity and the vast array of modes of operation that provide different types of chemical information. In particular, size-exclusion chromatography (SEC) [6] is often used to obtain the molecular-weight distribution, while the separation in liquid adsorption chromatography (LAC) depends on the FTD and CCD [7,8]. In addition, LC at critical conditions (LCCC) [5,9,10] is a powerful technique to determine the FTD by effectively 'switching off' the effect of molecular weight on the separation. Although the listed techniques are extremely useful, it is difficult to fully resolve the heterogeneity of a sample with a single one-dimensional separation technique. Furthermore, it can be difficult to relate different distributions (such as MWD and FTD) that are determined using diverse techniques.

By combining two separation modes, multidimensional characterization of molecular distributions can be achieved within a single analysis [11]. Two-dimensional LC techniques are effective for the characterization of complex mixtures in an industrial setting [12,13]. Such mixtures can be resolved by the appropriate selection of two very different ("orthogonal") separation dimensions, modulated *via* loop-based interfaces. The modulator collects fractions of the first-dimension (^{1}D) effluent and subsequently transfers these to the second-dimension (^{2}D) column. The separation is called comprehensive (LC × LC) if a constant fraction of the ^{1}D effluent is subjected to a ^{2}D separation and if the first-dimension separation is essentially preserved. Usually, the ^{2}D analysis time is equal to the modulation time.

Back in 1998, normal-phase (NP) LC × reversed-phase (RP) LC was performed for the separation of alkyl-alcohol ethoxylates [14]. The analytes were separated based on the number of polar EO groups under what are now known as hydrophilic-interaction-chromatography (HILIC) conditions. RPLC was used to separate different initiators based on their alkyl chain length. Nowadays, fast LC × LC separations with high peak capacities can be obtained by employing active modulation, as shown by Gargano et al. [15]. Moreover, appropriate selection of the HILIC and RPLC conditions allows for group-type separation of fatty-alcohol derivatives, while still providing separation based on EO content and alkyl chain length [16,17].

Although HILIC × RPLC has been reported numerous times for the separation of ethoxylates as discussed in the paragraph above, the complexity of the samples analyzed has remained relatively modest, with examples limited to alkyl alcohols or fatty acids ranging in alkyl chain-length from C_8 to C_{18}. Biobased initiator feedstocks, which are more sustainable than the common petroleum-derived initiators, are now being used for the production of polyether polyols. Due to the increased complexity of the initiator feedstock, such products demand LC × LC separations with higher resolution. An example is castor oil ethoxylates, which may contain ethoxylated fatty acids, such as linoleic (C18:2), oleic (C18:1), stearic (C18:0), and ricinoleic acid (C18:1-OH), as well as the mono-, di-, tri- and tetra-esters of these fatty acids [18]. The sample complexity includes (*i*) the degree of ethoxylation, (*ii*) the degree of saturation of C_{18} fatty acids, (*iii*) the formation of up to penta-esters resulting in structures with high carbon numbers and (*iv*) the presence of various positional isomers. Therefore, very efficient LC × LC separations are required to resolve such chemical features.

In addition to the separation of ethoxylates from a blended initiator feedstock, EO/PO triblock copolymers have been studied using LC × LC to determine their CCD. Jandera et al. [19] reported on an RPLC × HILIC separation of such polymers, while Malik et al. [20] coupled two LCCC interaction methods online for the separation of EO/PO copolymers. Although the principle of selective separations of EO/PO polymers has been demonstrated, only partial resolution was achieved in these studies. The LC × LC method described by Malik et al. demands a highly complicated setup, incorporating multiple trapping stages involving short RPLC columns during the modulation process. This yielded a ^{2}D LCCC separation time of 12 min, resulting in a long total analysis time.

In this work, we report on the development of an LC × LC method using ultra-high-pressure LC (UHPLC) technology and its application to highly complex polyether polyol samples. HILIC × RPLC methods have been developed for the separation of castor oil, reacted with different stoichiometric equivalents of EO. Hyphenation with high-resolution mass spectrometry (HRMS) allowed for a comprehensive characterization of various ethoxylated fatty acids, as well as the mono-, di-, tri-, tetra-, and penta-esters of various fatty acids, including positional isomers. These isomers were ultimately distinguished with the aid of MS/MS experiments. In addition, the LC × LC separation of a blended formulation is shown, featuring the group-type separation of glycerol ethoxylate, glycerol propoxylate, and glycerol ethoxylate-*random*-propoxylate copolymer, and allowing the CCD and MWD to be concurrently determined.

2. Experimental

2.1. Chemicals and samples

To study the separation of blended polyether polyols, glycerol ethoxylate (Gly-EO), glycerol propoxylate (Gly-PO), and glycerol ethoxylate-*random*-propoxylate copolymer (Gly-EO/PO) were used. Artificial formulations were created by mixing the aforementioned samples in different ratios. In addition, castor oil reacted with 20 mole equivalents ethylene oxide (COE-20) and with 40 mole equivalents (COE-40) were used. The samples were kindly supplied by Dow Benelux B.V. (Terneuzen, The Netherlands). Aqueous solutions were prepared using Milli-Q grade water (18.2 mΩ). The solvents used included acetonitrile (ACN, LC–MS grade) and methanol (MeOH, ULC/MS grade) obtained from Biosolve (Valkenswaard, The Netherlands). Ammonium formate and formic acid (reagent grade, ≥95%) were purchased from Sigma-Aldrich (Darmstadt, Germany). All materials were used as received, mobile phases were not filtered prior to use.

2.2. Instrumentation and analytical conditions

For one-dimensional LC method development, experiments were carried out by use of a Waters Acquity UPLC system (Waters, Milford, MA, USA). The system comprised of an Acquity UPLC binary solvent manager, sample manager, column manager and evaporative light-scattering detector (ELSD). To protect the first-dimension column, an Acquity UPLC in-line filter (Waters, 0.2 μm frit) was installed in front of the analytical column. Reversed-phase separations were carried out using a Zorbax RRHD Eclipse Plus C18 (50 mm × 2.1 mm I.D, 1.8 μm particle size) or an Acquity BEH Phenyl (50 mm × 2.1 mm I.D., 1.7 μm particle size) analytical column. HILIC experiments were performed using a Kinetex HILIC core-shell column (150 mm × 2.1 mm I.D., 2.6 μm particle size). Analytical conditions are supplied in Table 1.

LC × LC-HRMS experiments were performed using an Agilent 1290 infinity 2D-LC system (Agilent Technologies, Waldbronn, Germany). In the first dimension, a quaternary pump was installed, while the second dimension was equipped with a binary pump. Other modules included an autosampler, two thermostatted column compartments, the comprehensive 2D-LC option employing a 2-position/4-port duo valve, and an Agilent G6540B Q-TOF mass spectrometer. The valve was equipped with two 40-μL loops

Table 1
Analytical conditions used for one-dimensional LC method development.

	Blended polyether polyols		Castor oil ethoxylates (COE-20 & COE-40)	
	RPLC	HILIC	RPLC	HILIC
Injection volume	5.0 μL	2.0 μL	5.0 μL	2.0 μL
Sample concentration	1 mg/mL in MeOH	Gly-EO and Gly-EO/PO: 10 mg/mL in ACN Gly-PO: 1 mg/mL in ACN	1 mg/mL in MeOH	5 mg/mL in ACN
Column	Zorbax RRHD Eclipse Plus C18 (50 × 2.1 mm, 1.8 μm)	Phenomenex Kinetex HILIC (150 × 2.1 mm, 2.6 μm)	Acquity UPLC BEH Phenyl (50 × 2.1 mm, 1.7 μm)	Phenomenex Kinetex HILIC (150 × 2.1 mm, 2.6 μm)
Column Temp	23 °C	10 °C	23 °C	10 °C
Flow Rate	0.5 mL/min	0.1 mL/min	0.5 mL/min	0.4 mL/min
Mobile Phase A	Deionized Water (100%)	ACN (100%)	Deionized Water (100%)	ACN (100%)
Mobile Phase B	MeOH (100%)	10 mM ammonium formate, pH 3.2	ACN (100%)	10 mM ammonium formate, pH 3.2
Mobile Phase Gradient	Time (min): % B 0.0-0.5: 20% 0.5-3.0: 20-100% 3.0-6.0:100% 6.01-8.0: 20%	Time (min): % B 0.0-2.0: 10% 2.0-75.0: 10-35% 75.0-80.0: 35% 80.01-90.0: 10%	Time (min): % B 0.0-0.5: 20% 0.5-3.0: 20-100% 3.0-6.0: 100% 6.01-8.0: 20%	Time (min): % B 0.0-3.0: 5% 3.0-40.0: 5-50% 40.0-42.0: 50% 42.01-48.0: 5%
ELSD Conditions	ELSD: Waters Acquity UPLC Evaporative Light-Scattering Detector Nebulizer Temperature: Cooling; Drift Tube Temperature: 50 °C; Nebulizer Gas Pressure (Nitrogen): 40 psi; Gain: 500, 20 data points per second			

attached to two distinct multiple heart-cutting valves, which can be used for both multiple heart-cutting and comprehensive 2D-LC experiments. For negative ionization LC × LC-HRMS, 0.03 mL/min of 12.5% aqueous ammonium-hydroxide solution was added post column using a tee-connection *via* an Agilent 1260 series isocratic pump to enhance $[M-H]^-$ ion formation. The LC × LC system was controlled by OpenLAB CDS Chemstation version C01.07 SR2 [255], and the Q-TOF was controlled by MassHunter Acquisition software version B.05.01 Build 5.01.5125 (Agilent Technologies). Full method details of the different LC × LC-HRMS methods are shown in Table 2.

Exact mass LC–MS/MS spectra were acquired at collision energies of 20 eV and 35 eV after separation of COE-20 by the described one-dimensional HILIC method. Both targeted and non-targeted (auto) MS/MS experiments were performed with an isolation width of about 4 *m/z* units. In targeted MS/MS mode, the $[M + 2NH_4]^{2+}$ ions were specified as target masses.

2.3. Data treatment and compound identification

The one-dimensional LC-ELSD data were exported as space-separated files and processed using MatLab 2013a (Mathworks, Woodshole, MA, USA). LC × LC-HRMS data processing and analysis were performed using GC Image LC × LC-HRMS Edition Software (GC Image, Lincoln, NE, USA) and MassHunter Qualitative Analysis software [B.07.00] (Agilent Technologies). To identify compounds in the LC × LC-HRMS representations, the measured accurate mass and the isotope distribution of a given solute were compared to the theoretically expected values of the corresponding adduct. In addition, compounds were identified *via* the predicted chemical formula using the 'Find by Formula' data mining algorithm in the MassHunter Qualitative Analysis software.

3. Results and discussion

3.1. Method development for HILIC and RPLC separations

3.1.1. Blended polyether polyols

Fig. 1a shows an overlay of the HILIC separations obtained for Gly-EO, Gly-PO and Gly-EO/PO using a linear gradient from ACN to buffer (10 mM ammonium formate, pH 3.2). The retention was driven by the chain length of EO, such that retention time increases with degree of ethoxylation. The relatively hydrophobic Gly-PO has little interaction with the stationary phase and eluted in one single peak close to the unretained time, t_0, while Gly-EO and Gly-EO/PO were retained and resolved according to their ethoxylate distribution. For the Gly-EO polymer, isomer separation was observed, which was more pronounced in the low molecular weight range (see inset of Fig. 1a). Isomeric structures could be the result of incorporation of the same number of EO monomers over the three possible positions of the glycerol initiator. During the method optimization, we observed that besides the gradient slope, temperature played an important role in method optimization. In particular, cooling the analytical column to 10 °C (isothermal) was needed to resolve the high-molecular-weight fraction of the Gly-EO/PO according to the degree of ethoxylation (see Fig. S1 of Supporting information).

The same sample set was subjected to RPLC separations using fast gradients and short columns (L = 50 mm), developing methods compatible with LC × LC cycle times. As can be seen from Fig. 1(a and b), the selectivity of this separation is different from that of HILIC. In particular, Gly-PO was differentiated by the degree of propoxylation. The same was observed for the Gly-EO/PO sample, showing an additional distribution compared to the HILIC separation. Furthermore, the degree of ethoxylation for Gly-EO can be partially resolved under the given RP conditions according to carbon chain-length. However, such distributions can be easily suppressed by starting the gradient with a higher percentage of organic modifier or by choosing a stronger solvent (ACN instead of MeOH, data not shown).

Although powerful, the two methods were not capable (by themselves) of characterizing the interdependence of degree of propoxylation and ethoxylation. Moreover, when considering a blended formulation of the three samples, no single one-dimensional separation will be able to provide MWD and CCD information of all three polymers simultaneously.

3.1.2. Castor oil ethoxylates

Fig. 2a shows the chromatograms obtained for castor oil reacted with 20 and 40 mole equivalents EO under HILIC conditions. Similar chromatographic profiles were obtained for the COE-20 and COE-40 samples, although the latter elutes at higher retention times, showing predominant separation according to the degree

Table 2
Method parameters for LC × LC-HRMS separations.

LC × LC parameters	Blended polyether polyol	COE-20	COE-40
Injection			
Injection volume	1 μL	1 μL	1 μL
Sample concentration	A-1, A-2: 0.1 mg/mL A-3: 0.5 mg/mL in ACN	0.5 mg/mL in ACN	0.5 mg/mL in ACN
First Dimension			
Column	Phenomenex Kinetex HILIC (150 × 2.1, 2.6 μm)	Phenomenex Kinetex HILIC (150 × 2.1, 2.6 μm)	Phenomenex Kinetex HILIC (150 × 2.1, 2.6 μm)
Oven temperature	10 °C	10 °C	10 °C
Solvent A	10 mM ammonium formate, buffered to pH 3 with formic acid	10 mM ammonium formate, buffered to pH 3 with formic acid	10 mM ammonium formate, buffered to pH 3 with formic acid
Solvent B	Acetonitrile	Acetonitrile	Acetonitrile
Flow rate	0.027 mL/min	0.020 mL/min	0.020 mL/min
Gradient	0.0-4.0 min. 10% A 4.0–140 m in. 10–35% A 140.0–160.0 min. 35% A 160.01–200.0 min. 10% A	0.0-10.0 m in. 5% A 10.0–100 m in. 5–25% A 100.0–160.0 m in. 25–50% A 160.01–300.0 m in. 50% A 300.0–320.0 m in. 5% A	0.0–10.0 m in. 5% A 10.0–100 m in. 5–25% A 100.0–160.0 m in. 25–50% A 160.01–500.0 m in. 50% A 500.0–520.0 m in. 5% A
Modulation			
Switching valve	2 position/4 port duo valve	2 position/4 port duo valve	2 position/4 port duo valve
Loop size	40 μL	40 μL	40 μL
Modulation volume	21.6 μL	22 μL	22 μL
Modulation time	0.8 min	1.1 min	1.1 min
Second Dimension			
Column	Zorbax RRHD Eclipse Plus C_{18} (50 × 2.1, 1.8 μm)	Acquity UPLC BEH Phenyl (50 × 2.1 mm, 1.7 μm)	Acquity UPLC BEH Phenyl (50 × 2.1 mm, 1.7 μm)
Oven temperature	50 °C	50 °C	50 °C
Solvent A	0.1% ammonium formate in H_2O	0.1% ammonium formate in H_2O	0.1% ammonium formate in H_2O
Solvent B	0.1 % ammonium formate in methanol	Acetonitrile	Acetonitrile
Flow rate	1.0 mL/min	1.2 mL/min	1.2 mL/min
Gradient	0.0–0.05 min: 50%B 0.06–0.65 min: 70-90%B 0.66–0.80 min. 50% B	0.0–0.01 min: 50–70% B 0.01–0.75 min: 70–100% B 0.75–0.85 min: 100% B 0.86–1.1 m in. 50% B	0.0–0.01 min: 50–70% B 0.01–0.75 min: 70–100% B 0.75–0.85 min: 100% B 0.86–1.1 min. 50% B
Detection MS			
Model	Agilent MS Q-TOF G6540B		
Ion source	Dual Jet Stream Electrospray Ionization (AJS ESI)		
Ion polarity	Positive		
Drying gas	325 °C, 13 L/min		
Nebulizer	0.4 MPa		
Sheath gas	400 °C, 12 L/min		
Capillary voltage	3500 V		
Nozzle voltage	1000 V		
Scan range	100–3000 *m/z*		
Scan rate	2.00 spectra/s		
Reference masses pos. ESI	*m/z* 121.050873, $(C_5H_5N_4)^+$, *m/z* 922.009798, $(C_{18}H_{19}O_6N_3P_3F_{24})^+$		
Negative ionization			
Ion polarity	Negative		
Post column make-up flow	0.03 mL/min, 12.5% aqueous ammonium hydroxide to enhance $(M\text{-}H)^-$ ion formation		
Reference masses	*m/z* 119.036320, $(C_5H_3N_4)^-$, *m/z* 966.000725, $(C_{19}H_{19}O_8N_3P_3F_{24})^-$		

of ethoxylation. A high number of features corresponding to ethoxylated distributions were eluted throughout the entire chromatogram, while the unreacted free fatty acids eluted at the beginning of the chromatogram (confirmed by HILIC-HRMS and discussed further in Section 3.2.2). Base-line separation for the studied samples was not achieved due to the high sample complexity, which may be explained by a certain degree of selectivity for variations in the carbon chain length of the various esters present, as well as the presence of isomeric distributions.

To obtain an orthogonal separation mechanism, RPLC separations using a C_{18} column were initially investigated. While many features could be separated using this method, a portion of the solutes was too strongly retained and eluted isocratically at 100% organic modifier using either ACN or MeOH (data not shown). For LC × LC methods, it is preferred to elute the analytes within the gradient to avoid wrap-around between runs [21,22]. Therefore, alternative column chemistries for RPLC with lower lipophilicity were evaluated, and the resulting chromatograms using a phenyl-hexyl column employing fast gradients are given in Fig. 2b. The elution of the hydrophilic PEG and Gly-EO (t_R 0–1.5 min) differs between the two samples due to variation in molecular weights (increased MW for COE-40). For COE-20 and COE-40, the separation profiles of the ethoxylated fatty acids, mono-, di-, tri-, tetra- and penta-esters (t_R 1.5–3.5 min) showed great similarity, independent of degree of ethoxylation, indicating so-called "pseudocritical conditions" [23,24].

3.2. LC × LC-HRMS

Based on the one-dimensional method development for both the formulated polyether polyol and castor oil ethoxylates, HILIC was coupled to the corresponding RPLC methods in the LC × LC experiments. To identify all the separated species and to provide information on the MWD and CCD, the separation was coupled to

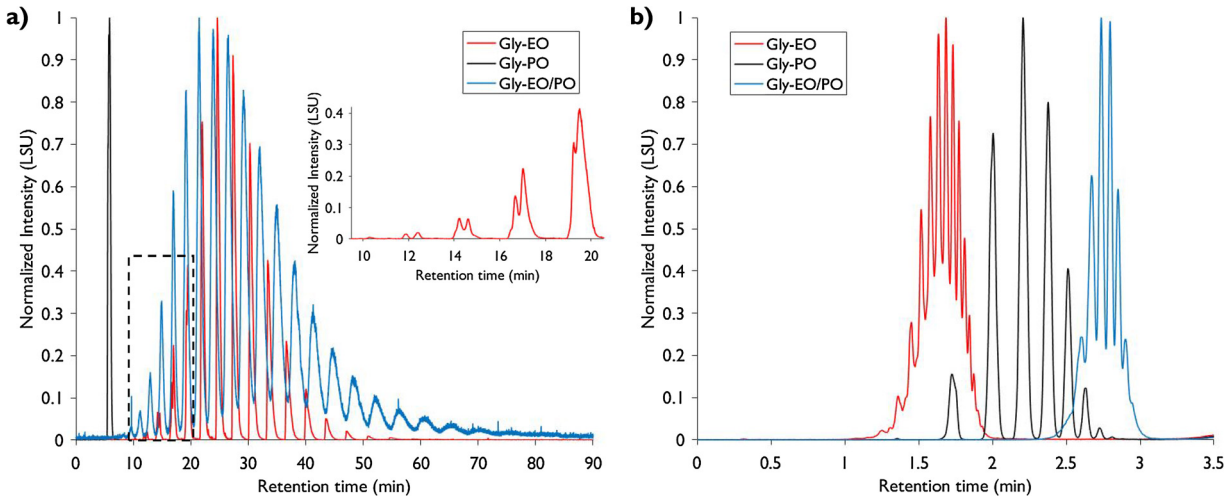

Fig. 1. HILIC-ELSD (a) and RPLC-ELSD (b) separations of glycerol ethoxylate (Gly-EO, red line), glycerol propoxylate (Gly-PO, black) and glycerol ethoxylate-*random*-propoxylate copolymer (Gly-EO/PO, blue). HILIC separation was according to degree of ethoxylation while the RPLC separation yielded distributions according to carbon chain-length (Gly-EO) and degree of propoxylation. For the Gly-EO polymer, isomer separation was observed as shown in the inset (a). For detailed chromatographic conditions, see the Experimental Section and Table 1. (For interpretation of the references to colour in this figure legend, the reader is referred to the web version of this article.)

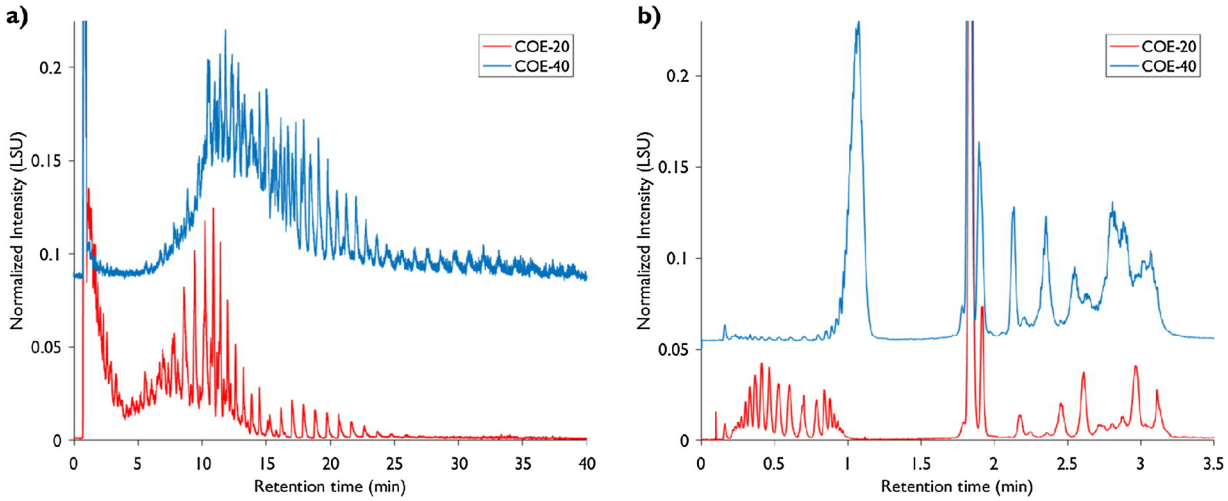

Fig. 2. HILIC-ELSD (a) and RPLC-ELSD (b) separations of castor oil ethoxylates reacted with 20 (COE-20, red lines) and 40 (COE-40, blue lines) mole equivalents of EO monomers. The HILIC separation was mainly governed by the degree of ethoxylation, while the RPLC separation was according to carbon chain length and degree of saturation of various ethoxylated (polymerized) free fatty acids. For detailed chromatographic conditions, see the Experimental Section and Table 1. (For interpretation of the references to colour in this figure legend, the reader is referred to the web version of this article.)

high-resolution mass spectrometry. Due to the use of ^{2}D columns with a 2.1 mm I.D., flow rates were maintained relatively low (maximum of 1.2 mL/min) compared to more commonly used 4.6 mm I.D. columns. This allowed for the direct coupling of the ^{2}D effluent to the MS without splitting the flow to waste. The latter is a common practice in LC × LC—MS. Compounds were identified based on their accurate masses and isotope distributions (measured *versus* theoretical).

3.2.1. *LC × LC-HRMS polyether polyol formulation*

Fig. 3 shows the LC × LC-HRMS total-ion chromatogram (TIC) of a synthetic formulation containing Gly-EO, Gly-PO and Gly-EO/PO. The three different glycerol-based polyols were clearly clustered in different regions of the LC × LC separation space, showing a clear group-type separation, whilst allowing speciation based on degree of ethoxylation and /or propoxylation. Gly-PO eluted with little to no interaction from the HILIC column, but was separated into individual peaks in the ^{2}D RPLC dimension. As indicated in the LC × LC plot, partial breakthrough of the low molecular weight portion (n_{PO} = 5–9) of the polymer was observed in the ^{2}D [25]. This is explained by the relatively large amount of strong solvent (ACN) present in the collected fractions that were subsequently injected onto the ^{2}D in combination with the relatively large volume fractions (21.6 μL) injected (approximately 20% of the ^{2}D column void). While these factors increase the chance of breakthrough, the majority of the Gly-PO was effectively trapped at the head of the column and eluted as a function of the applied gradient. Therefore, the higher MW portion of Gly-PO (n_{PO} = 10–15) was not present in the breakthrough peak. Along the *x*-axis of the LC × LC plot, Gly-EO constituents were separated based on the degree of ethoxylation in the HILIC dimension. Again, partial breakthrough in the ^{2}D for Gly-EO was observed since high volume fractions of ACN were transferred to the ^{2}D. As the ACN fraction of the ^{1}D effluent decreases with increasing retention time due to the gradient applied in the ^{1}D, the retention of the retained peak increased. This was confirmed by an additional injection study showing the partial breakthrough

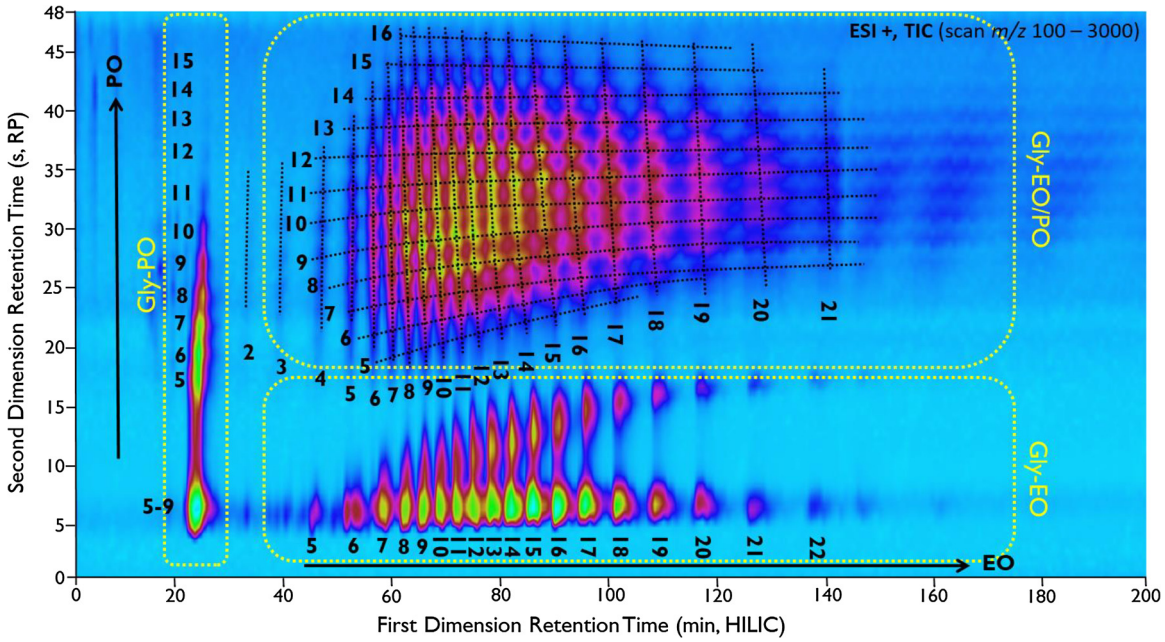

Fig. 3. HILIC × RPLC-(+)HRMS total-ion chromatogram (TIC) of a formulation consisting of glycerol-initiated ethoxylate (Gly-EO), propoxylate (Gly-PO) and ethoxylate-*random*-propoxylate copolymer (Gly-EO/PO). Group-type separation between the different polymer classes was obtained, whilst allowing for the molecular weight and chemical composition distribution to be determined. Monomer sequences of each polymer were identified using the MS data which are shown in the figure. For detailed chromatographic conditions, see the Experimental Section and Table 2.

effect as function of the initial percentage of organic modifier used for the ^{2}D RPLC separation and the fraction of ACN present in the injection solvent (see Fig. S2 of the Supplementary information). Furthermore, these injection studies showed that even with low injection volumes (2 μL) breakthrough still occurred, so lowering the ^{1}D flow rate would not be an effective measure. In addition, changing the initial modifier concentration led to an increase in the retained signals for Gly-EO. However, the breakthrough issues (Fig. S2) could not be fully overcome. Recent work on active solvent modulation to improve solvent compatibility [26,27] could be an interesting strategy, but this was found to be out of scope of this current study. This could be addressed in upcoming work. The majority of the separation space was occupied by the speciation of the Gly-EO/PO random copolymer. While the polymer was resolved according to the degree of ethoxylation under HILIC conditions, an additional distribution in propoxylation was achieved for every given EO number. Effective focusing of the Gly-EO/PO solutes was achieved under the applied ^{2}D gradient conditions, starting from 50% B to 70% B in 0.01 min, while the PO distribution was resolved under linear gradient conditions (70–90% MeOH in 0.60 min). Therefore, the large-volume fractions injected did not cause distortion of the ^{2}D separation, and a clear representation of the apparent composition of the random copolymer was obtained. The composition of each peak is indicated in the LC × LC plot.

A straightforward HILIC × RPLC method was achieved with high orthogonality and a moderate peak capacity of roughly 550, as calculated for Gly-EO_6/PO_9. An approximate value of the peak capacity is provided. In a specific LC × LC separation this peak capacity may not be used to full, due to limited coverage of the separation space. The separation exhibits a high degree of orthogonality (degree of ethoxylation resolved independently of degree of propoxylation) and most of the separation space is efficiently used to resolve the complexity of the sample.

The molecular weight of the analyzed samples was up to 2000 Da. However, higher EO numbers could be resolved in a similar system by applying a gradient to higher percentages of aqueous buffer, while conversely, higher PO numbers could be resolved using a stronger solvent (such as ACN) as the organic modifier for the ^{2}D RPLC separations.

3.2.2. LC × LC-HRMS of castor oil ethoxylates

Fig. 4 depicts the TIC plot of a HILIC × RPLC-HRMS separation of COE-20 using positive-mode ESI. For each distribution present in the LC × LC chromatogram, HRMS was used to elucidate the chemical composition and degree of ethoxylation. Identifications were made by comparing the measured accurate mass and isotope distribution to the theoretical values for a given compound.

The major compounds observed are in agreement with Nasioudis et al. [18] and were identified as poly(ethylene glycol) (PEG), glycerol ethoxylate, ethoxylated series of ricinoleic, linoleic, oleic and stearic acids (Ric/Lin/Ole/Ste-*n*EO), and glycerol ethoxylate mono-, di-, tri-, tetra, and penta-esters of Ric/Lin/Ole/Ste (Gly-Ric_W/Lin_X/Ole_Y/Ste_Z-*n*EO) where W, X, Y, Z = 0, 1, 2, 3, 4 or 5 and $W+X+Y+Z=5$. The identifications of these ethoxylated series in the two-dimensional separation space are listed in Fig. 4.

The complexity of the COE-20 sample is clearly presented by the two-dimensional separation. As observed previously, the separation in the ^{1}D HILIC dimension was predominantly governed by degree of ethoxylation, whilst the ^{2}D RPLC dimension separated the solutes according to the hydrophobicity of the fatty acids incorporated in the various series. Hence, the hydrophilic PEG and glycerol ethoxylates were eluted first in the ^{2}D, followed by the mono-, di-, tri-, tetra-, and penta-esters as function of increasing RPLC retention. Within such ester-classes, the fatty acids were further separated according to equivalent carbon number (ECN), resulting in the separation of ricinoleate, linoate, oleate, and stearate

$$^{2D}n \approx {}^{1}n \cdot {}^{2}n \approx \left(\frac{{}^{1}t_G}{1.7 \cdot {}^{1}w_{0.5h}} + 1\right) \cdot \left(\frac{{}^{2}t_G}{1.7 \cdot {}^{2}w_{0.5h}} + 1\right) \approx \left(\frac{136}{1.7 \cdot 1.6} + 1\right) \cdot \left(\frac{0.65}{1.7 \cdot 0.04233} + 1\right) \approx 550$$

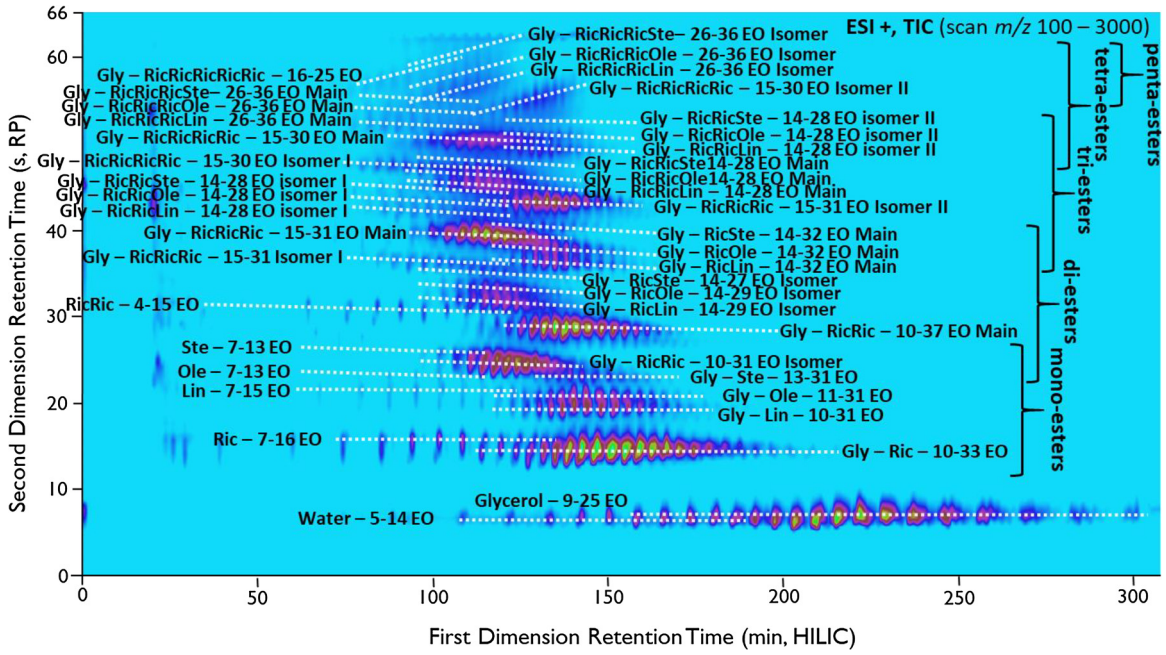

Fig. 4. HILIC × RPLC-(+)HRMS separation of the castor oil ethoxylate (COE-20). The ^{1}D HILIC dimension (horizontal) indicates the degree of ethoxylation, while the ^{2}D RPLC column (vertical) separates the ethoxylated species according to hydrophobicity. Various ethoxylated fatty acids, as well as glycerol ethoxylated mono-, di-, tri-, tetra- and penta-esters were identified using the obtained accurate mass and isotope distributions. These species are indicated in the figure, as well as their degree of ethoxylation. For detailed chromatographic conditions, see the Experimental Section and Table 2.

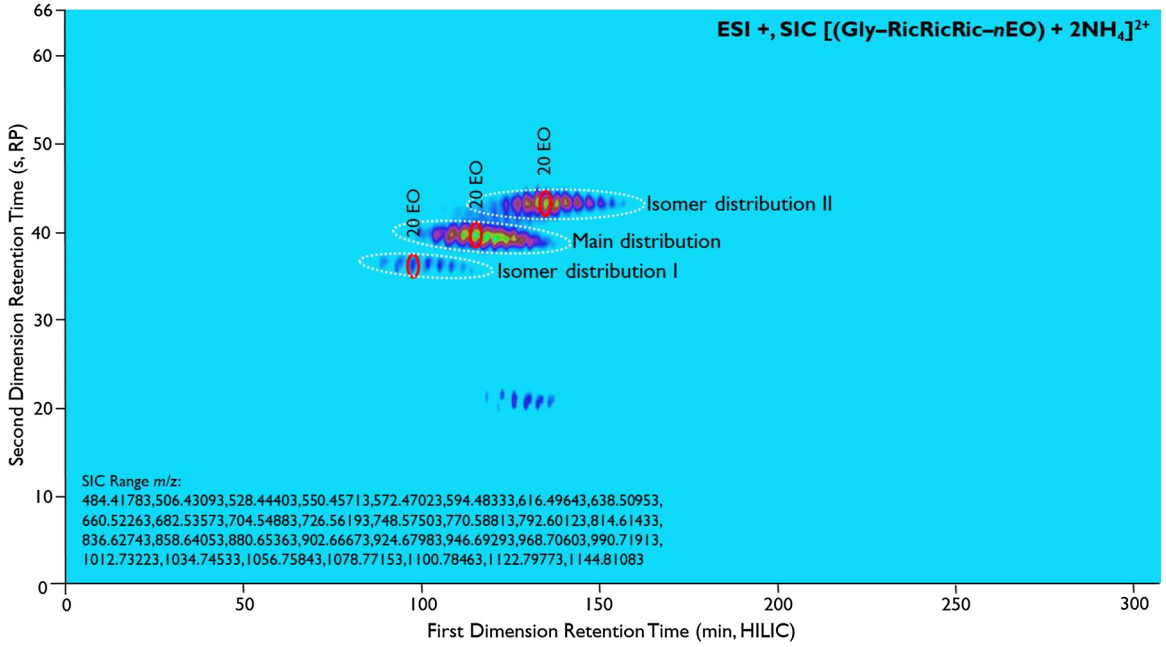

Fig. 5. LC × LC-(+)HRMS selected-ion chromatogram (SIC) of the doubly charged ammonia adducts of glycerol ethoxylate triricinoleate [Gly-RicRicRic-nEO + 2NH$_4$]$^{2+}$ showing three different isomer distributions (white dotted ellipses). The highlighted peaks in the chromatogram (red ellipses) all have the same degree of ethoxylation (EO = 20) with the same accurate mass and isotope distribution, confirming them as isomers. These isomers were subjected to LC–MS/MS experiments to elucidate the structural differences, shown in Fig. 6. (For interpretation of the references to colour in this figure legend, the reader is referred to the web version of this article.)

species with increasing retention time. For example, this can be clearly observed for glycerol ethoxylate mono-Ric/Lin/Ole/Ste with similar EO numbers, which stacked on top of each other in the separation space (Fig. 4). Although hydrophilic Gly-EO and PEG are present in this LC × LC separation, these do not show breakthrough as observed in Fig. 3 for the blended polyether polyol sample. Important differences exist between the two methods, specifically in the experimental conditions for the second dimension. For the separation of COE-20 a phenyl column is used while the organic modifier is ACN (stronger solvent) compared to a C_{18} stationary phase with MeOH as organic modifier for the blended polyether polyol sample. Under the applied conditions, Gly-EO and PEG are not retained at all on the RP column and eluted at the dead time of the ^{2}D separation. However, the desired information is obtained (separation of degree of ethoxylation in HILIC dimensions) and the peaks provided clean mass spectra (no other breakthrough signals

Table 3
Identified compounds in LC × LC-HRMS analysis of castor oil ethoxylated with 20 and 40 mole equivalents of EO.

Series	Name	20 EO mole equivalent		40 EO mole equivalent	
		Degree of ethoxylation	Mass range (MW)	Degree of ethoxylation	Mass range (MW)
1	Polyethylene glycol	5-14	238.14–634.38	5-28	238.14–1250.74
2	Glycerol ethoxylate	9-26	488.28–1236.73	20-33	972.57– 1544.91
3	Monoricinoleate ethoxylate	7-16	606.43–1002.67	5-25	518.38–1398.91
4	Monolinoleate ethoxylate	7-15	588.42–940.63	5-24	500.37–1336.87
5	Monooleate ethoxylate	7-13	590.44–854.60	5-25	502.39–1382.91
6	Monostearate ethoxylate	7-13	592.46–856.61	5-24	504.40–1340.90
7	Glycerol ethoxylate monoricinoleate	10-33	812.55–1825.15	22-44	1358.90–2327.47
8	Glycerol ethoxylate monolinoleate	10-31	794.54–1719.09	17-42	1102.72–2203.38
9	Glycerol ethoxylate monooleate	11-31	840.58–1721.11	19-42	1192.79–2205.39
10	Glycerol ethoxylate monostearate	13-30	930.65–1679.09	19-42	1194.81–2207.41
11	Diricinoleate ethoxylate	0-15	578.49–1238.88	4-21	754.60–1503.04
12	Monoricinoleate-monolinoleate	0	560.48	–	–
13	Monoricinoleate-monooleate	0	562.50	–	–
14	Monoricinoleate-monostearate	0	564.51	–	–
15-16	Glycerol ethoxylate diricinoleate + isomer	10–37	1092.79–2281.50	18–41	1445.00–2457.60
17-18	Glycerol ethoxylate monoricinoleate-monolinoleate + isomer	14–32	1250.88–2043.36	19–42	1471.02–2483.62
19-20	Glycerol ethoxylate monoricinoleate-monooleate + isomer	14–32	1252.90–2045.37	19–42	1473.03–2485.63
21-22	Glycerol ethoxylate monoricinoleate-monostearate + isomers	14–29	1254.92–1915.31	19-42	1475.05 – 2487.65
23	Triricinoleate ethoxylate	0–4	858.73–1034.84	–	–
24	Diricinoleate-monolinoleate	0	840.72	–	–
25	Diricinoleate-monooleate	0	842.74	–	–
26	Diricinoleate-monostearate	0	844.75	–	–
27-29	Glycerol ethoxylate triricinoleate + isomer I + isomer II	14–31	1549.14–2297.58	20–40	1813.29 – 2693.82
30-32	Glycerol ethoxylate diricinoleate-monolinoleate + isomer I + isomer II	14–28	1531.12–2147.49	20–40	1795.28–2675.81
33-35	Glycerol ethoxylate diricinoleate-monooleate + isomer I + isomer II	14–28	1533.14 – 2149.51	20-40	1797.30 – 2677.82
36-38	Glycerol ethoxylate diricinoleate-monostearate + isomer I + isomer II	14–28	1535.16–2151.52	20–40	1799.31–2679.84
39-41	Glycerol ethoxylate tetraricinoleate + isomer I & Isomer II	15–30	1873.40–2533.79	20–40	2093.53–2974.06
42-43	Glycerol ethoxylate triricinoleate-monolinoleate + isomer	26–36	2339.68–2779.94	25–41	2295.65–3000.07
44-45	Glycerol ethoxylate triricinoleate-monooleate + isomer	26–36	2341.70–2781.96	25–41	2297.67–3002.09
46-47	Glycerol ethoxylate triricinoleate-monostearate + isomer	26–36	2343.71–2783.97	25–41	2299.68–3004.10
48	Glycerol ethoxylate pentaricinoleate	16–25	2197.67–2593.90	–	–

from different species were found to be present in these peaks). Therefore, we found the use of these conditions acceptable.

For glycerol ethoxylated di-esters, similar elution profiles were observed as described above, resulting in the detection of glycerol ethoxylate monoricinoleate-Ric/Lin/Ole/Ste. However, when analyzing the separated distributions, isomer distributions (same exact mass and isotope distribution) became apparent for each glycerol ethoxylate di-ester at each level of ethoxylation. These isomer distributions were grouped together with both reduced ^{1}D HILIC and ^{2}D RPLC retention compared to the main di-ester distributions (most abundant species). The same observations were made when analyzing glycerol ethoxylate tri- and tetra-esters. Apart from the main distributions of glycerol ethoxylate diricinoleate-Ric/Lin/Ole/Ste, two isomer distributions were observed for each species. Again, the isomer distributions were grouped and both reduced and increased retention in the ^{1}D HILIC and ^{2}D RPLC separation dimensions were observed with respect to the main distribution. Fig. 5 presents the isomer distributions of glycerol ethoxylate triricinoleate in a selected-ion LC × LC-HRMS plot. This clearly shows the effect of HILIC × RPLC selectivity for the isomers. The presence of such isomers may possibly be ascribed to the incorporation of the various fatty acids at different positions of the glycerol initiator. To study this hypothesis, MS/MS experiments were performed (see Section 3.3).

In addition to the HILIC × RPLC-(+)HRMS separation described above, the same separation was repeated using negative-ion ESI in order to detect additional species with low ionization efficiencies in the positive-ion mode. In Fig. S3 (Supplementary material), a selected-ion LC × LC-(-)HRMS plot is shown indicating the identified negatively charged ions. Esterified fatty acids were detected with little or no degree of ethoxylation, resulting in unretained elution from the HILIC dimension. However, these compounds were resolved in the ^{2}D (RPLC) according to hydrophobicity, as previously discussed. Detected species include ricinoleic acid, diricinoleate, monoricinoleate-monolinoleate, monoricinoleate-monooleate, monoricinoleate-monostearate, triricinoleate, diricinoleate-monolinoleate, diricinoleate-monooleate and diricinoleate-monostearate.

Furthermore, HILIC × RPLC experiments were conducted on a castor oil sample ethoxylated with 40 mole equivalent EO (COE-40) to study the separation capabilities of the method using a sample with a higher EO load, and thus increased hydrophilicity and higher molecular weights. In the first dimension, a longer isocratic hold at 50% buffer was incorporated to ensure elution of the solutes with increased polarity, while maintaining the same ^{2}D conditions as were used for COE-20. In doing so, the HILIC dimension was capable of resolving species with a higher degree of ethoxylation, while maintaining the speciation capabilities of the ^{2}D RPLC dimension, as shown in Fig. S4 (Supplementary material).

The findings from the above-discussed HILIC × RPLC separations in both positive and negative ESI mode for COE-20 and COE-40 samples are summarized in Table 3. In total, 48 different ethoxylated distributions were detected in a mass range of 238–3004 Da, with the majority of these species having a degree of ethoxylation up to 20. An estimated peak capacity of around 900 was obtained for the COE-20 separation, calculated based on the average width of the three isomer peaks of Gly-RicRicRic-20EO.

$$ {}^{2D}n \approx {}^{1}n \cdot {}^{2}n \approx \left(\frac{{}^{1}t_g}{{}^{1}w}\right) \cdot \left(\frac{{}^{2}t_g}{{}^{2}w}\right) \approx \left(150/3.167\right) \cdot \left(0.75/0.040\right) \approx 900 $$

This allowed for speciation of mono-, di-, tri-, tetra- and penta-esters with varying fatty-acid compositions in combination with the separation of various isomeric ethoxylated distributions. The HILIC separation was also extended to accommodate the separation of castor oil ethoxylates with a higher degree of ethoxylation, while the speciation capabilities of the ^{2}D RPLC separation were maintained.

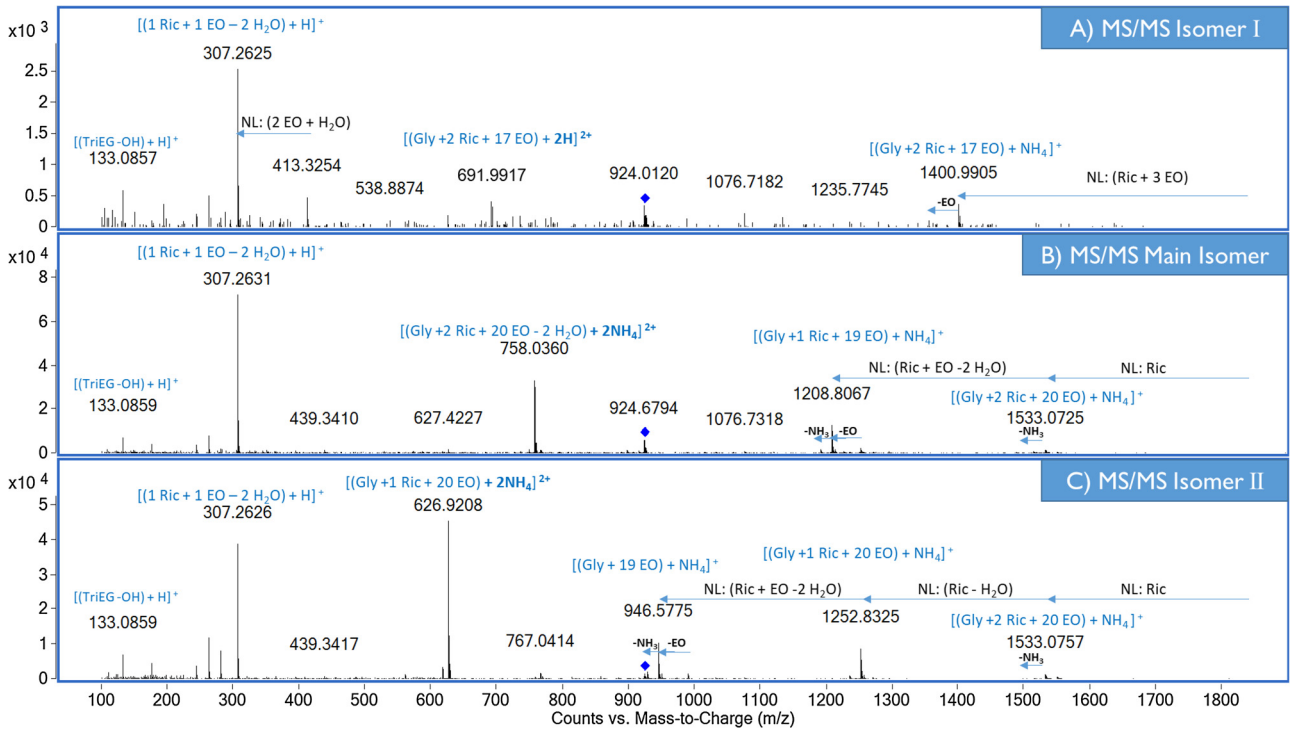

Fig. 6. MS/MS spectra of three different isomer precursor ions [Gly-RicRicRic-20EO + $2NH_4$]$^{2+}$ showing distinct fragmentation patterns. Neutral losses (NL) and identified fragment ions are shown in the corresponding spectra. Proposed fragmentation pattern of the three different isomers are shown in Fig. 7. For detailed conditions for MS/MS measurements, see the Experimental Section.

When compared with conventional LC–MS analysis, the presented LC × LC methods were found to be crucial for the complete characterization of complex COEs. Since the complexity of the sample was fully resolved in the chromatographic domain, clean and easily interpretable mass spectra were obtained that were specific to a single compound. In contrast, one-dimensional LC–MS provides overlapping charge distributions of multiple compounds, which can result in extremely complicated mass-spectra and compositional assignments. Furthermore, the LC × LC approach minimizes discrimination effects in ionization efficiency, thus increasing the accuracy of quantification and enhancing the detectability of low-abundant species. Ultimately, the HILIC × RP separations may be hyphenated with other detectors, such as an ELSD or a charged-aerosol detector (CAD), for quality-control or process-control analyses. Full characterization of the resulting data can be performed by translating the LC × LC-HRMS chromatograms with known identifications to LC × LC templates for peak-pattern matching [28].

3.3. LC–MS/MS of castor oil ethoxylate isomers

As shown in Section 3.2.2, during the HILIC × RPLC-HRMS analysis, multiple distributions were identified as having the same elemental composition. Such isomer distributions had significantly different chromatographic properties when compared to the main distributions, as shown in Fig. 5 for glycerol ethxoylate triricinoleate. The substantially different elution profiles suggested the incorporation of the fatty acid moieties at different positions in the molecule, generating positional isomers. To study the structural differences between the positional isomers, accurate-mass LC—MS/MS experiments were performed. Glycerol ethoxylate mono-, di- and tri-ricinoleate and their isomer(s) with a fixed EO number of 20 were subjected to MS/MS analysis to compare fragmentation patterns. In addition, the isomeric specie(s) of glycerol ethoxylate monolinoleate, glycerol ethoxylate monolinoleate-monoricinoleate and glycerol ethoxylate monolinoleate-diricinoleate were subjected to MS/MS measurement to compare their fragmentation patterns with compounds containing solely ricinoleate moieties. The MS/MS spectra of the main and two isomer peaks of [Gly-RicRicRic-20EO + $2NH_4$]$^{2+}$ (corresponding to series 27–29 in Table 3) are shown in Fig. 6.

The MS/MS spectra of [Gly-Lin-20EO + $2NH_4$]$^{2+}$, the main and isomer peak of [Gly-RicLin-20EO + $2NH_4$]$^{2+}$, and the main and two isomer peaks of [Gly-RicRicLin-20EO + $2NH_4$]$^{2+}$ (corresponding to series 8, 17–18 and 30–32 in Table 3, respectively) are shown in the Supplementary information, Fig. S5. The identification of the observed neutral losses and fragment ions are depicted in the corresponding MS/MS spectra. As can be seen in Fig. 6, distinct spectra were obtained with different fragmentation patterns for the three Gly-RicRicRic-20EO isomers. The MS/MS spectrum of isomer II (Fig. 6c) showed consecutive neutral losses of 298.2505, 280.2432 and 306.2550 Da, which were identified as ricinoleic acid, (ricinoleic acid – H_2O) and (ricinoleic acid + EO – $2H_2O$), respectively. The observed neutral losses indicate that three ricinoleic acid molecules were esterified and situated at the terminal position of one of the ethoxylated glycerol arms. This is supported by the work of Nasioudis et al. [18], who observed similar characteristic neutrals losses of 298 and 280 for esterified ricinoleic acids. The single EO unit on the most internal ricinoleic acid is most likely positioned at the ester bond and not ethoxylated at the secondary OH group. Support for this hypothesis is given by the observation of a similar neutral loss of (linolenic acid + EO – H_2O) for Gly-Lin-20EO shown in Fig. S5a (Supplementary information), which does not contain a secondary OH group on the fatty-acid moiety. A different fragmentation pattern was observed for the main peak of Gly-RicRicRic-20EO (Fig. 6b). Again, consecutive neutral losses of 298.2537 and 324.2658 Da were observed, identified as ricinoleic acid and (ricinoleic acid + EO – H_2O). In contrast with the MS/MS spectrum of isomer II, the subsequent loss of a third ricinoleic acid moiety was not observed. The observed

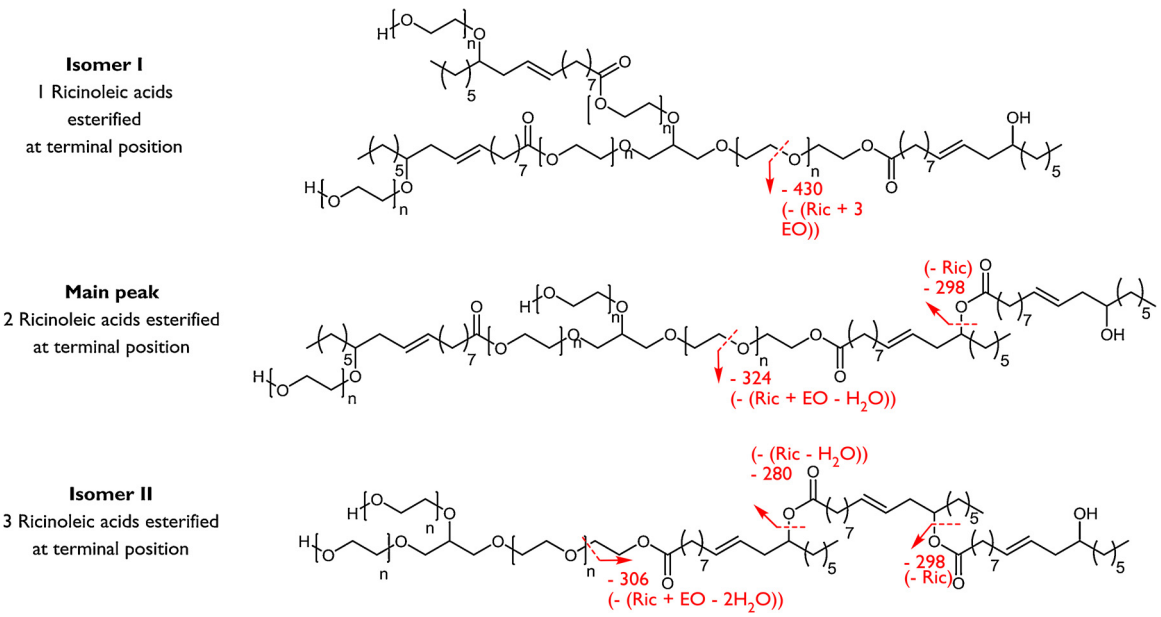

Fig. 7. Proposed fragmentation pattern of the observed isomers for Gly-RicRicRic-20EO based on the consecutive neutrals losses as shown in the MS/MS spectra of Fig. 6. The nominal masses of the proposed consecutive neutral losses are included as well as their annotation. The position (specific arm of the glycerol initiator) of the internal ricinoleic acid units is not known, but structures have been drawn for illustrative purposes.

neutral losses suggest that two ricinoleic acids were esterified and positioned at the terminal position of an ethoxylated arm of the glycerol initiator, while the third ricinoleic acid may be internally positioned in the same glycerol arm or situated internally within another arm of the ethoxylated glycerol initiator. The ion intensity of isomer I (Fig. 6a) was at least one order of magnitude lower compared to the other two MS/MS spectra. This is also observed in the LC × LC plot, where the peak intensity was significantly lower. It is not known at this stage whether the lower intensity is caused by differences in reaction kinetics of the three isomers or by a lower ionization efficiency. Nevertheless, valuable information could be retrieved from the MS/MS spectra. It should, however, be noted that the observed intensities were approaching the noise-level. A neutral loss of 430.3357 Da was observed and identified as (ricinoleic acid + 3 EO), which was also confirmed by the observation of the fragment ion *m/z* 691.9917, characterized as Gly-RicRic-17EO. Consecutive neutral losses of other ricinoleic acid units were not observed, suggesting that for isomer I, a single ricinoleic acid was externally positioned, while the other two fatty acid moieties were situated internally. Proposed structures of the isomers are shown in Fig. 7, including proposed fragmentation patterns that explain the observed neutral losses.

The proposed structural differences between the main and isomer peaks of Gly-RicRicRic-20EO explain the observed retention differences in the two-dimensional chromatograms. The three esterified ricinoleic acid units at the external position, as suspected for isomer II, may increase hydrophobic interaction in the ^{2}D RPLC, due to less steric hindrance of the hydrophilic ethoxylate part of the molecule. At the same time, this may allow greater accessibility of the hydrophilic ethoxylates to interact with the ^{1}D HILIC stationary phase. This behavior (both increased HILIC and RPLC retention times) was observed for isomer II compared to the main peak, which was suspected to have only two esterified ricinoleic acids situated at the external position. The internal fatty-acid unit may cause steric hindrance of the ethoxylates, reducing hydrophilic interaction in the ^{1}D dimension and simultaneously reducing RPLC interaction. The same trend was observed for isomer I, with further reduction of the HILIC and RPLC retention, which may be explained by the presence of just a single ricinoleic acid at the external position.

4. Conclusion

In this paper the use of comprehensive two-dimensional liquid chromatography for the separation of highly complex polyether polyols was demonstrated. High orthogonality was achieved between the first hydrophilic-interaction-chromatography dimension and the second reversed-phase dimension, separating species based on the degree of ethoxylation and the degree of propoxylation or alkyl chain-length, respectively. By using 2.1-mm I.D. columns in the second dimension, the separation could be hyphenated with high-resolution mass spectrometry without the need for flow-splitting prior to introduction into the MS. For a blended formulation, group-type separation between glycerol ethoxylate, glycerol propoxylate and glycerol ethoxylate-*random*-propoxylate copolymer was achieved, allowing for both the molecular-weight and chemical-composition distributions to be obtained, revealing the apparent composition of the formulation.

For castor oil reacted with different mole equivalents of ethylene oxide, a highly efficient second dimension RPLC separation was developed, capable of resolving various mono-, di-, tri-, tetra- and penta-esters consisting of ricinoleate, oleate, linoleate, stearate, and combinations of such fatty acids. The di-, tri- and tetra-ester species showed the presence of isomer distributions with significant differences in LC × LC retention. LC—MS/MS analysis of such isomers showed different fragmentation patterns with characteristic neutral losses of the fatty acid moieties, indicating the terminal or internal positioning of the alkyl chains. Such positional differences could explain the observed chromatographic behavior of the isomers.

Acknowledgments

This publication has been written as part of the Open Technology Programme (IWT-STW collaboration), project number 14624 (DEBOCS), which is financed by the Netherlands Organization

for Scientific Research (NWO). Andrea Gargano acknowledges the NWO-VENI grant IPA (722.015.009) for funding.

Appendix A. Supplementary data

Supplementary material related to this article can be found, in the online version, at doi:https://doi.org/10.1016/j.chroma.2018.07.054.

References

[1] M.F. Sonnenschein, Polyurethanes: Science, Technology, Markets, and Trends, first ed., Wiley, New York, 2015, http://dx.doi.org/10.1002/9781118901274.
[2] M. Ionescu, Chemistry and Technology of Polyols for Polyurethanes, first ed., Rapra Tech., Shrewsbury, UK, 2005, http://dx.doi.org/10.1002/pi.2159.
[3] N. Makhiyanov, D.K. Safin, An NMR study of the structure and molecular characteristics of polyether block copolymers based on propylene oxide and ethylene oxide, Polym. Sci. Ser. B 48 (2006) 37–45, http://dx.doi.org/10.1134/S1560090406010088.
[4] R. Chen, A.M. Tseng, M. Uhing, L. Li, Application of an integrated matrix-assisted laser desorption/ionization time-of-flight, electrospray ionization mass spectrometry and tandem mass spectrometry approach to characterizing complex polyol mixtures, J. Am. Soc. Mass Spectrom. 12 (2001) 55–60, http://dx.doi.org/10.1016/S1044-0305(00)00200-2.
[5] J.R. Stutzman, M.C. Crowe, J.N. Alexander, B.M. Bell, M.N. Dunkle, Coupling charge reduction mass spectrometry to liquid chromatography for complex mixture analysis, Anal. Chem. 88 (2016) 4130–4139, http://dx.doi.org/10.1021/acs.analchem.6b00485.
[6] M.C. van Engelen, R.A. Salome, H. Eghbali, M.N. Dunkle, J.R. Stutzman, E.P.C. Mes, Coupling size-exclusion chromatography to mass spectrometry for the analysis of low-molecular-weight polymers: a versatile tool to study complex polyether polyol formulations, LC-GC Eur. 30 (2017) 178–187.
[7] B. Trathnigg, M.I. Malik, N. Pircher, S. Hayden, Liquid chromatography at critical conditions in ternary mobile phases: gradient elution along the critical line, J. Sep. Sci. 33 (2010) 2052–2059, http://dx.doi.org/10.1002/jssc.201000181.
[8] S. Abrar, B. Trathnigg, Characterization of polyoxyethylenes according to the number of hydroxy end groups by hydrophilic interaction chromatography at critical conditions for polyethylene glycol, Anal. Bioanal. Chem. 400 (2011) 2531–2537, http://dx.doi.org/10.1007/s00216-010-4448-3.
[9] S. Abrar, B. Trathnigg, Analysis of polyethyleneoxide macromonomers by liquid chromatography along the critical adsorption line, Anal. Bioanal. Chem. 400 (2011) 2577–2586, http://dx.doi.org/10.1007/s00216-010-4554-2.
[10] R. Epping, U. Panne, J. Falkenhagen, Critical conditions for liquid chromatography of statistical copolymers: functionality type and composition distribution characterization by UP-LCCC/ESI-MS, Anal. Chem. 89 (2017) 1778–1786, http://dx.doi.org/10.1021/acs.analchem.6b04064.
[11] P. Schoenmakers, P. Aarnoutse, Multi-dimensional separations of polymers, Anal. Chem. 86 (2014) 6172–6179, http://dx.doi.org/10.1021/ac301162b.
[12] M. Pursch, S. Buckenmaier, Loop-based multiple heart-cutting two-dimensional liquid chromatography for target analysis in complex matrices, Anal. Chem. 87 (2015) 5310–5317, http://dx.doi.org/10.1021/acs.analchem.5b00492.
[13] D.R. Stoll, P.W. Carr, Two-dimensional liquid chromatography: a state of the art tutorial, Anal. Chem. 89 (2017) 519–531, http://dx.doi.org/10.1021/acs.analchem.6b03506.
[14] R.E. Murphy, M.R. Schure, J.P. Foley, One- and two-dimensional chromatographic analysis of alcohol ethoxylates, Anal. Chem. 70 (1998) 4353–4360, papers2://publication/uuid/16E8088C-AE2C-4D40-84EE-0926D50854FC.
[15] A.F.G. Gargano, M. Duffin, P. Navarro, P.J. Schoenmakers, Reducing dilution and analysis time in online comprehensive two-dimensional liquid chromatography by active modulation, Anal. Chem. 88 (2016) 1785–1793, http://dx.doi.org/10.1021/acs.analchem.5b04051.
[16] V. Elsner, S. Laun, D. Melchior, M. Köhler, O.J. Schmitz, Analysis of fatty alcohol derivatives with comprehensive two-dimensional liquid chromatography coupled with mass spectrometry, J. Chromatogr. A 1268 (2012) 22–28, http://dx.doi.org/10.1016/j.chroma.2012.09.072.
[17] V. Elsner, V. Wulf, M. Wirtz, O.J. Schmitz, Reproducibility of retention time and peak area in comprehensive two-dimensional liquid chromatography, Anal. Bioanal. Chem. 407 (2015) 279–284, http://dx.doi.org/10.1007/s00216-014-8090-3.
[18] A. Nasioudis, J.W. Van Velde, R.M.A. Heeren, O.F. Van den Brink, Detailed molecular characterization of castor oil ethoxylates by liquid chromatography multistage mass spectrometry, J. Chromatogr. A 1218 (2011) 7166–7172, http://dx.doi.org/10.1016/j.chroma.2011.08.032.
[19] P. Jandera, J. Fischer, H. Lahovská, K. Novotná, P. Česla, L. Kolářová, Two-dimensional liquid chromatography normal-phase and reversed-phase separation of (co)oligomers, J. Chromatogr. A 1119 (2006) 3–10, http://dx.doi.org/10.1016/j.chroma.2005.10.081.
[20] M.I. Malik, S. Lee, T. Chang, Comprehensive two-dimensional liquid chromatographic analysis of poloxamers, J. Chromatogr. A 1442 (2016) 33–41, http://dx.doi.org/10.1016/j.chroma.2016.03.008.
[21] D.R. Stoll, J.D. Cohen, P.W. Carr, Fast, comprehensive online two-dimensional high performance liquid chromatography through the use of high temperature ultra-fast gradient elution reversed-phase liquid chromatography, J. Chromatogr. A 1122 (2006) 123–137, http://dx.doi.org/10.1016/j.chroma.2006.04.058.
[22] B.W.J. Pirok, A.F.G. Gargano, P.J. Schoenmakers, Optimizing separations in online comprehensive two-dimensional liquid chromatography, J. Sep. Sci. (2017) 1–30.
[23] X. Jiang, P.J. Schoenmakers, X. Lou, V. Lima, J.L.J. Van Dongen, J. Brokken-Zijp, Separation and characterization of functional poly(n-butyl acrylate) by critical liquid chromatography, J. Chromatogr. A 1055 (2004) 123–133, http://dx.doi.org/10.1016/j.chroma.2004.08.136.
[24] A.V. Gorshkov, H. Much, H. Becker, H. Pasch, V.V. Evreinov, S.G. Entelis, Chromatographic investigations of macromolecules in the “critical range” of liquid chromatography. I. Functionality type and composition distribution in polyethylene oxide and polypropylene oxide copolymers, J. Chromatogr. A 523 (1990) 91–102, http://dx.doi.org/10.1016/0021-9673(90)85014-M.
[25] X. Jiang, A. Van Der Horst, P.J. Schoenmakers, Breakthrough of polymers in interactive liquid chromatography, J. Chromatogr. A 982 (2002) 55–68, http://dx.doi.org/10.1016/S0021-9673(02)01483-8.
[26] M. Pursch, A. Wegener, S. Buckenmaier, Evaluation of active solvent modulation to enhance two-dimensional liquid chromatography for target analysis in polymeric matrices, J. Chromatogr. A 1562 (2018) 78–86, http://dx.doi.org/10.1016/j.chroma.2018.05.059.
[27] D.R. Stoll, K. Shoykhet, P. Petersson, S. Buckenmaier, Active solvent modulation: a valve-based approach to improve separation compatibility in two-dimensional liquid chromatography, Anal. Chem. 89 (2017) 9260–9267, http://dx.doi.org/10.1021/acs.analchem.7b02046.
[28] S.E. Reichenbach, P.W. Carr, D.R. Stoll, Q. Tao, Smart Templates for peak pattern matching with comprehensive two-dimensional liquid chromatography, J. Chromatogr. A 1216 (2009) 3458–3466, http://dx.doi.org/10.1016/j.chroma.2008.09.058.